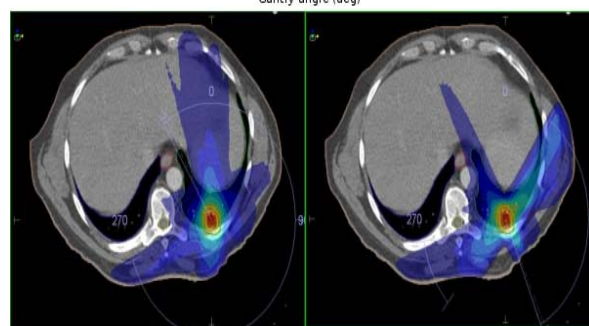
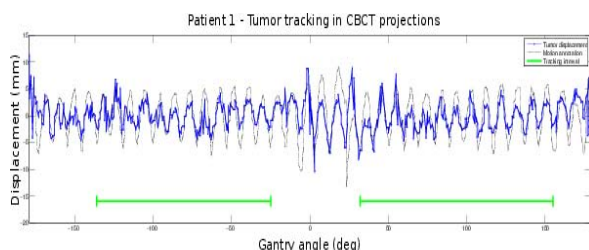


Tracking angles (deg)				Used arc ranges (deg)		PTV volume (cc)		DVH parameters							
								Lung V13.4Gy (V20Gy EQD2)		Spinal cord D0.1cc (EQD2, $\alpha/\beta=2$ )		Esophagus D0.1cc (EQD2, $\alpha/\beta=2$ )			
Patient	AP	PA	U	L	U	L	U	L	U	L	U	L	U	L	
1	136	25	32	155	285	185	19.7	15.4	5.08	5.94	5.70	5.50	3.00	11.30	
2	160	65	20	108	NA	NA	NA	NA	NA	NA	NA	NA	NA	NA	
3	141	48	52	149	160	93	27.4	23.7	5.94	7.00	3.70	20.40	5.50	9.70	
4	135	51	66	127	160	84	13.2	11.4	8.40	10.00	14.90	5.70	23.30	10.90	
5	180	0	0	180	245	245	33.2	32.9	17.07	16.23	2.00	2.80	12.20	8.30	



**Conclusion:** The results indicate the feasibility of VMAT treatments under tumor tracking for selected patients. The arcs available for planning influence the quality of treatment. The L partial arc plans had clinically acceptable quality in four patients. Treatments with reduced margins could be safely delivered by gating the treatment beam if the tumor motion exceeds the margins. Also, a great advantage is that the dose delivered to the tumor could be exactly monitored.

#### OC-0211

##### Real-time MRI-guided Radiotherapy for pancreatic cancer

S.A. Rosenberg<sup>1</sup>, A. Wojcieszynski<sup>1</sup>, C. Hullett<sup>1</sup>, M. Geurts<sup>1</sup>, S.J. Lubner<sup>2</sup>, N.K. LoConte<sup>2</sup>, D.A. Deming<sup>2</sup>, D.L. Mulkerin<sup>2</sup>, C.S. Cho<sup>3</sup>, S.M. Weber<sup>3</sup>, E. Winslow<sup>3</sup>, K.A. Bradley<sup>1</sup>, J. Bayouth<sup>1</sup>, P.M. Harari<sup>1</sup>, M.F. Bassetti<sup>1</sup>

<sup>1</sup>University of Wisconsin, Department of Human Oncology, Madison, USA

<sup>2</sup>University of Wisconsin, Division of Hematology and Oncology-Department of Medicine, Madison, USA

<sup>3</sup>University of Wisconsin, Division of Surgical Oncology-Department of Surgery, Madison, USA

**Purpose or Objective:** Pancreatic cancer with vascular involvement has a poor prognosis regardless of treatment. The toxicity of chemoradiation to adjacent normal organs can contribute to treatment discontinuation and adverse outcomes in some patients. We hypothesized that real-time MRI guided radiotherapy for borderline or locally advanced pancreatic carcinoma would enable safer treatment delivery with tight margins and diminished normal tissue toxicity than conventional treatment approaches.

**Material and Methods:** Patients with borderline or locally advanced pancreatic cancer were eligible for evaluation for MRI-guided radiotherapy. Patients underwent complete staging, including baseline CA19-9 and triple phase CT imaging. Patients underwent simulation with an inhale breath hold 3D and cine scans on a MRI Guided Treatment Planning

system. Locoregional lymph node coverage was incorporated at the discretion of the Radiation Oncologist. The mean CTV to PTV expansion was 3 mm (range 2-5 mm). The primary GTV was tracked in real-time throughout treatment and the PTV or similar structure was used as a boundary for triggering treatment. A patient initiated repeated breath hold strategy was used to increase the reproducibility and duty cycle of radiotherapy.

**Results:** We have completed treatment for our first 5 patients with borderline or locally advanced pancreatic adenocarcinoma. The population was 4:1 Male:Female with a mean age of 61.8 years (range 52-67). All patients had an elevated CA19-9 at presentation, with a mean of 714 U/mL (range 62 - 2350 U/mL). Locoregional lymphatics were treated in 4/5 patients. The mean PTV was 222.7 cc (range 40.3-346.4 cc). The PTV was treated to 50.4 Gy at 1.8 Gy per a fraction with concurrent chemotherapy for all patients. With a median follow-up of 166 days (range 50 - 278 days), an average 66% reduction in CA19-9 1-2 months following chemoradiation was observed. The OS is 60% at time of follow up. One grade 4 toxicity was observed with duodenal ulceration during radiotherapy requiring hospitalization. The number of patients, overall survival, local control, progression free survival, and changes in CA19-9 levels will be updated at the time of presentation.

**Conclusion:** Real-time MRI-guided radiotherapy enables the design and delivery of highly conformal treatment for patients with borderline or locally advanced pancreatic carcinoma. A significant reduction in CA19-9 levels after treatment was observed. Real time MR imaging throughout treatment enables high precision tracking to minimize treatment margins and normal tissue dose exposure. MRI-guided radiotherapy may provide opportunities for normal organ toxicity reduction and future dose escalation strategies.

#### OC-0212

##### Liver motion tracking using optical flow cine-MRI registration

M. Seregini<sup>1</sup>, C. Paganelli<sup>1</sup>, P. Summers<sup>2</sup>, M. Bellomi<sup>2</sup>, G. Baroni<sup>1</sup>, M. Riboldi<sup>1</sup>

<sup>1</sup>Politecnico di Milano, Dipartimento di Elettronica-Informazione e Bioingegneria, Milano, Italy

<sup>2</sup>Istituto Europeo di Oncologia, Department of Radiology, Milano, Italy

**Purpose or Objective:** The development of radiotherapy treatment units with integrated MRI scanners is stimulating interest in fully MRI-guided treatment protocols. Cine-MRI sequences capable of acquiring 5-6 2D images per second are already available, thus providing a potential means of non-invasive, online motion monitoring with high soft-tissue contrast. This work investigates the feasibility of liver motion tracking using optical flow registration of Cine-MR images series.

**Material and Methods:** Liver cine-MRI series (balanced steady-state free precession, 256x256 pixel, 1.28x1.28mm spacing,  $f = 3.3\text{Hz}$ ) providing 220 images over a 70s scan were acquired in 25 patients and 5 healthy volunteers after informed consent. Ground-truth liver motion consisted in the trajectories of numerous sparse features ( $P_{\text{SIFT}}$ ) extracted using a previously tested algorithm based on the Scale Invariant Feature Transform (SIFT) [1]. For each subject, optical flow (OF) registration, as proposed in [2], was applied between the first image of the series and each subsequent frame, thus obtaining time-resolved dense motion fields [Fig. 1]. Trajectories based on OF ( $P_{\text{OF}}$ ) were then derived by applying these motion fields to the positions of the SIFT features detected in the first image. To assess the accuracy of the motion fields, the 2D frame-by-frame distances ( $D_{\text{SIFT-OF}}$ ) between  $P_{\text{SIFT}}$  and  $P_{\text{OF}}$  were calculated for every trajectory and, for each subject, their distributions were described with median, inter-quartile range, 5<sup>th</sup> and 95<sup>th</sup> percentiles. Linear correlation coefficients ( $r_{\text{SIFT-OF}}$ ) between